Polymer 51 (2010) 240–248

Contents lists available at ScienceDirect

Polymer

journal homepage: www.elsevier.com/locate/polymer

Study on the thermal-induced shape memory effect of pyridine containing supramolecular polyurethane

Shaojun Chen, Jinlian Hu*, Haitao Zhuo, Chunwah Yuen, Laikuen Chan

Institute of Textiles and Clothing, The Hong Kong Polytechnic University, Hung Hom, Kowloon, Hong Kong, China

ARTICLE INFO

Article history:
Received 29 July 2009
Received in revised form
28 September 2009
Accepted 15 November 2009
Available online 20 November 2009

Keywords:
Shape memory
Polymer
Supramolecular structure

ABSTRACT

In this paper, a series of pyridine containing supramolecular polyurethanes (PUPys) were synthesized from BINA, HDI and BDO. Then the structure, morphology and thermal-induced shape memory effect (SMEs) of PUPys were investigated systematically. Results show that strong hydrogen bonding is formed in the urethane group as well as in the pyridine ring; and phase separation consisting of soft phase and hard phase occurs in the PUPy. In addition, it is found that the lower limit of BINA content for PUPys exhibiting good SMEs is 30 wt%. PUPys with higher BINA content show higher shape fixity, higher shape recovery and better strain stability. Moreover, the shape recovery force increases with the decreasing of BINA content. Finally, the temperature-dependent FT-IR spectra support that the hydrogen bonding in the pyridine ring serves as the molecular switch; while the hydrogen bonding in the urethane groups acts as the physical netpoints for the utilization of PUPys as SMMs.

1. Introduction

Polymeric materials are called shape memory polymers (SMPs) if they have the capability of fixing a temporary shape and recovering to their original shape upon application of an external stimulus like heat, light *etc.* [1,2]. Shape memory effect (SME) is the basic properties of SMPs. According to the stimulus, SMEs are divided into thermal-induced SMEs [3,4], light-induced SMEs [5] and electro-active SMEs [6]. There are also reports about magnetically induced SMEs [7] and water-driven SMEs [8]. Among them, thermal-induced SMEs are more common where the shape recovery takes place with respect to a certain critical temperature [1]. Since the first discovery of SMPs under the trade name of polynorborene in 1984, thermal-induced SMPs have drawn increasing attention because of their scientific and technological significance [1]. Various kinds of polymers like polyacrylate copolymers, polynorbornenes, segmented polyurethanes and cross-linked polyethylenes were developed to show SMEs. Especially, shape memory polyurethane (SMPU) composed of hard segment and soft segment has been extensively researched [9–11].

SMPU is usually synthesized from the long chain polyols, diisocyanate and short chain extenders. So far, the reported typical polyols includes PCL, PTMG, PBA, PHA, PLA [1]. Examples of hard segment include MDI/BDO, HDI/4,4-dihydroxylbiphenyl, MDI/BEBP or BHBP, MDI/DMPA [1]. In the common segmented SMPU, phase-separation structure consisting of hard domains and soft domains was microscopically observed [12]. It is generally accepted that hard segments can bind themselves via hydrogen bonding or crystallization making the SMPU very solid below melting temperature (T_m). Reversible phase transformation of soft segment either amorphous phase or semi-crystalline phase is reported to be responsible for the thermal-induced SMEs of SMPU. Thus, the SMEs of traditional SMPU can be controlled through the selection of molecular weight of soft segment, mole ratio between hard segment and soft segment, and polymerization process [13].

On the other hand, in addition to T_g-type-SMPs with amorphous switching segment and T_m-type-SMPs with crystalline switching segment [1,2], supramolecular SMPs based on thermal-reversible non-covalent bonding recently have been another new kind of SMPs [14]. In this system, the reversible non-covalent interactions are used to stabilize mechanically strain stated in polymer elastomers; and shape recovery is achieved upon heating due to the dissociation of non-covalent bonds. Examples of supramolecular SMPs may include hydrogen-bonded semi-interpenetration networks (semi-IPNs) [9,15,16]; PEG-α-CD supramolecular SMP networks [14,17]; supramolecular SMPs containing ureidopyridinone (UPy) side-groups [18]. Most recently, novel supramolecular SMPUs were also achieved in our group by grafting the UPy unit to the elastic polyurethane [19]. Moisture-sensitive SME was also observed in the pyridine containing supramolecular

* Corresponding author. Tel.: +852 2766 6437; fax: +852 2773 1432.
E-mail address: tchujl@inet.polyu.edu.hk (J. Hu).

0032-3861/$ – see front matter © 2009 Elsevier Ltd. All rights reserved.
doi:10.1016/j.polymer.2009.11.034

polyurethane networks [20]. In the previous literatures, it was reported that higher recovery rate was achieved when poly (ethylene glycol) (PEG) with higher molecular weight was introduced into the P(AA-co-MMA) networks, and the reversible phase transformation was responsible for the SMEs in the hydrogen-bonded PEG/P(AA-co-MMA) semi-IPN [16]. In addition, in the polymer networks containing a small fraction (ca. 2 mol%) of UPy pendant side-groups, the shape recovery and the sample's viscosity strongly depend on the temperature; and the H-bond dissociation dynamics strongly influence mechanical relaxation. They suggested that a high fraction of H-bonding side group might provide a better SME [18]. In an earlier communication, we had reported another kind of new supramolecular polyurethane networks containing large fraction of pyridine moieties for shape memory materials (SMMs) [20,21]. However, thermal-induced SMEs of pyridine containing polyurethanes (PUPys) have not been reported systematically until now. There are still no reports to explain the relationship of SMEs with the non-covalent bonds in previous literatures [17–19].

Therefore, in this study, a series of PUPys with various BINA contents were synthesized with N,N-bis (2-hydroxylethyl) isonicotinamine (BINA), hexamethylene diisocyanate (HDI) and 1,4-butanediol (BDO). Firstly, the morphology of PUPy with various BINA contents was investigated by FT-IR, DSC and DMA. Secondly, the shape memory properties particularly thermal-induced SMEs of PUPys were reported by comparing with SMEs of Tg-type-SMPU and Tm-type-SMPU; and the influence of BINA contents on shape fixity, shape recovery, shape stability, thermal-dependent shape recovery and shape recovery force were investigated systematically. Finally, the mechanism of thermal-induced SME was also explained.

2. Experimental part

2.1. Materials

Extra-pure-grade HDI, BINA and BDO (all from Sigma–Aldrich Chemical Co., St. Louis, MO) were used directly; and dimethylformamide (DMF) (from Ajax Finechem Ltd., Auckland, New Zealand) was dehydrated with 4-Å molecular sieves for several days before its use as a solvent.

2.2. Synthesis of PUPy

The compositions of PUPy with various BINA contents are provided in Table 1; and the synthesis routine of PUPy is presented in Scheme 1. The reaction to prepare the PUPy with various BINA contents was carried out in a 500-ml flask filled with nitrogen and equipped with a mechanical stirrer, a thermal meter, and a condenser. Firstly, BINA powder and DMF was added to the flask according to the composition as given in Table 1. After the BINA was dissolved completely under the mechanical stirring, HDI and 0.02 wt% catalyst (Dibutyltin dilaurate) were added to the flask. Then the reaction started immediately, and the viscosity was observed to increase significantly. After 2 h, BDO was added to the reaction; and the reaction was kept for another 4 h. To control the viscosity of solution, 10 ml DMF each was added into the reaction occasionally during the reaction process. Finally, 10 wt% PUPy/DMF solution was obtained. After casting on the PTFE mould and putting on the 100 °C oven for 12 h, film of PUPy with various BINA content were prepared. Before testing, the samples were dried in 100 °C vacuum again for 12 h. Sample in this study was coded as PUPy**, where the "**" delegates the BINA content, e.g. PUPy40.

Table 1
Composition of PUPy with various BINA contents.

Samples	BINA (g)	HDI (g)	BDO (g)	BINA (wt%)	HDI (wt%)	M_n ($\times 10^4$)	PDI
PUPy53	5.24	4.52	0	53.7	46.3	15.38	1.63
PUPy45	4.50	5.22	0.66	43.3	50.3	10.37	1.63
PUPy40	4.00	5.40	1.00	38.5	51.9	8.63	1.31
PUPy30	3.00	5.80	1.60	28.8	55.8	6.35	1.39
PUPy20	2.00	6.22	2.23	19.1	59.5	11.16	1.63
PUPy10	1.00	6.63	2.86	9.5	63.2	9.54	1.49

M_n is the number-average molecular weight; PDI is the polydispersity index.

2.3. Characterization

FT-IR spectra were recorded with a Nicolet 760 FT-IR spectrometer. 10 scans at 4 cm^{-1} resolution were signal averaged and stored as data files for further analysis; and smooth polymer film with a thickness of 0.2 mm were scanned by the FT-IR attenuated total reflection (ATR) method.

For the temperature-dependent FT-IR spectra, dried thin SMPU film was held between two pieces of KBr Plate and placed into a temperature-variable unit connected to the numerical temperature controller (Model WNMN, available from Science Equipment Company of Hong Kong). The temperature of thin film was monitored by a copper-constantan thermocouple held directly on the sample between the two salt plates. FT-IR spectra at various temperatures were recorded after each temperature was held constant for 20 min.

DSC testing was carried out by using Perkin-Elmer DSC-7 at a heating rate of 10.0 °C/min and a cooling rate of 10.0 °C/min under N_2.

In the dynamical mechanical analysis (DMA), specimens were cut from film with thickness of 0.2 mm, and the distance between two clamps is 15 mm in the initial testing status. Specimens were determined by using a Perkin–Elmer DMA at 1.0 Hz and a heating rate of 3.0 K/min.

Thermal-induced SMEs were characterized with thermal–mechanical testing, which was done by using an instron 4466 apparatus with a temperature-controlled chamber; and a personal computer was used to control and record all date [10]. The standardized film size was 5×20 mm^2 and the thickness was 0.2 mm. Specimens were firstly heated to $T_{high} = 60$ °C within 600 s. Then the sample was stretched to $\epsilon_m = 100\%$ elongation at T_{high} with 10 mm/min stretching rate. After that, cool air was introduced to the chamber for cooling sample film with constant strain $\epsilon_m = 100\%$ elongation to $T_{low} = 20$ °C within 900 s. Thereafter, the strain was released from ϵ_m to 0 and the temperature was recurrent raised to 80 °C for 600 s. That was one cycle among all cyclic tensile tests. The cycle for each sample was repeated four or five times for assessing the thermal-induced SMEs. Finally, the shape fixity (R_f) and shape recovery (R_r) were calculated according to the method of literature [1].

Thermal–strain recovery testing was performed in a microscopy (Leitz Wetzlar) with a hot stage (Mettler Toledo FP90 Central Processor & FP82 Hot Stage) and a camera (Pixera PVC 100C). The heating rate of the recovery measurement was 2 °C/min; and the length of specimen is recorded on heating process at the temperature range from 25 °C to 100 °C. Then the shape recovery (R_T), maximum shape recovery (R_{max}), shape fixity (F), shape stability (S) were calculated according to the method of literature [22].

3. Results and discussions

3.1. Structure of PUPy

Fig. 1 presents the FT-IR spectra of PUPy with various BINA contents. According to the composition given in Table 1, it is known

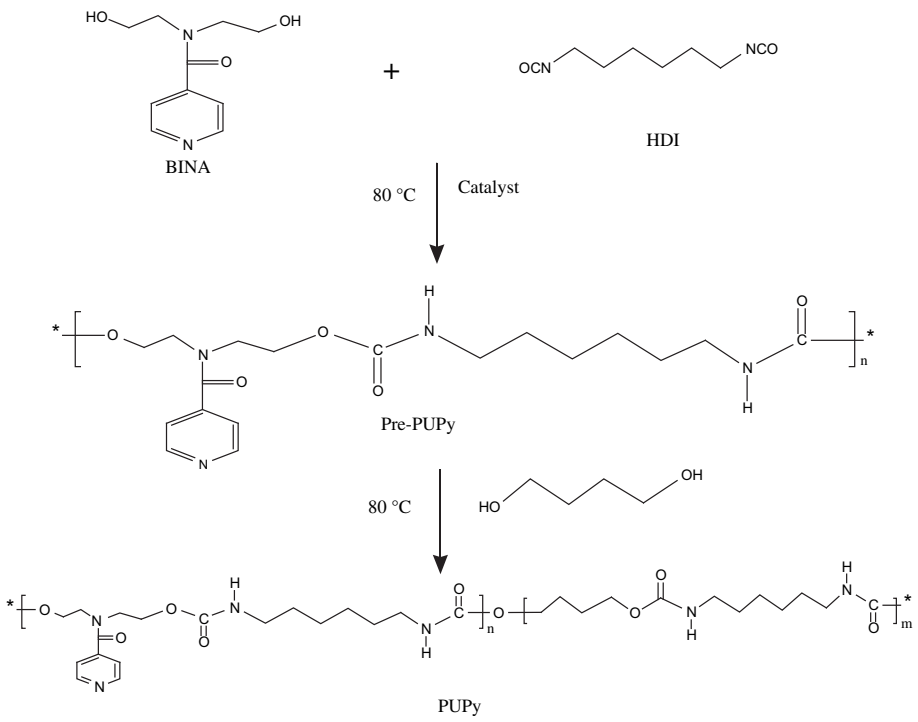

Scheme 1. The synthesis routine for PUPy with various BINA contents.

that the BINA content, reflecting the pyridine ring fraction, decreases with the increasing of BDO content; while the HDI content, reflecting the urethane group fraction, increases with the decreasing of BINA content. Thus, in Fig. 1(a), it can be found that the band density at 3313–3320 cm^{-1} for N–H stretching vibration of urethane group increases as the BINA content decreases. In contrast, the band density at about 3059 cm^{-1} for C–H stretching vibration of pyridine ring decreases with the decreasing of BINA content. In Fig. 1(b), it also can be found that the density at about 1635 cm^{-1} for C═O stretching vibration as well as at about 1600 cm^{-1} for C–N–C stretching vibration decreases significantly as the BINA content decreases. They even tend to be overlapped by C═O stretching vibration of urethane group due to its very low fraction of BINA in the spectrum of PUPy10. It implies that the fraction of hydrogen bonding in the urethane group increases with the decreasing of BINA content; while the fraction of hydrogen bonding in the pyridine ring decreases with the decreasing of BINA content.

In addition, it is also observed that the N–H stretching vibration of urethane group shifts from 3320 cm^{-1} to 3312 cm^{-1}; and the C═O stretching vibration of urethane group shifts from 1696 cm^{-1} to 1680 cm^{-1} as the BINA content decreases. In contrast, the C═O stretching vibration beside pyridine ring shifts from 1628 cm^{-1} to 1638 cm^{-1} though it tends to disappear in the spectrum of PUPy10. Moreover, in Fig. 1(c), it is also found that as the BINA content decreases, the out of plane CH deformation vibrations of pyridine ring shifts from 832 cm^{-1} to 834 cm^{-1}. In previous literatures [23,24], it was widely reported that hydrogen-bonded vibration would appear at the lower frequency for N–H vibration and C═O vibration; while the associated-pyridine ring shows a high breathing vibration frequency. It is generally accepted that the frequency shift is a measure of strength of hydrogen bonding [23]. Thus, these results indicate that as the BINA content decreases, the strength of hydrogen bonding in the urethane group gets stronger; in contrast, the strength of hydrogen bonding in the pyridine ring gets weaker.

3.2. Thermal properties of PUPy

In the segmented polyurethanes, due to the thermodynamic incompatibility between soft segment and hard segment, microphase separation occurs and results in hard segment-rich and soft segment-rich soft matrix [12,13]. Even though the phase separation is influenced by many factors, such as chemical composition, sequence length of the hard segment, and hydrogen bonding. It is generally accepted that the hydrogen bonding in the polyurethane is very closely related to the phase separation [25]. In the PUPy, it is confirmed above that high fraction of strong hydrogen bonding is formed between the N–H and C═O of urethane groups as well as between NH of urethane group and pyridine ring. Thus, the thermal-properties of PUPy may be influenced greatly by the hydrogen bonding.

Fig. 2 presents the DSC curves of PUPy with various BINA contents. In the first heating curves as shown in Fig. 2(a), it can be observed that in addition to the slight glass transition at the low temperature range, there is also broad high temperature transition with a big ΔC_p in the sample PUPy53. Robert *et al.* suggested that three characteristic endoderm transitions observed at temperature of 60–80 °C, 120–180 °C, and above 200 °C were correlated respectively with the short-range, long-range and microcrystalline ordering of hard segment units [26]. Therefore, the high temperature transition in this PUPy system should result from the long-range disorder hard-segment unit which is formed through the strong hydrogen bonding among urethane groups [27]. As the BINA content decreases, the high temperature transition tends to be a crystal melting peak. Moreover, the peak temperature moves to high temperature. On the second heating curves, this tendency gets clearer. In Fig. 2(b), it is found that the glass transition temperature (T_g) appears at ca. 55.4 °C in the PUPy53; ca. 43.8 °C in the PUPy40, and ca. 33.7 °C in the PUPy30. That is, the T_g decreases as the BINA content decreases. In addition, it can also be observed that PUPy20 and PUPy10 show big crystal melting peaks at 148.2 °C and at 163.7 °C respectively; while no clear glass transition is determined

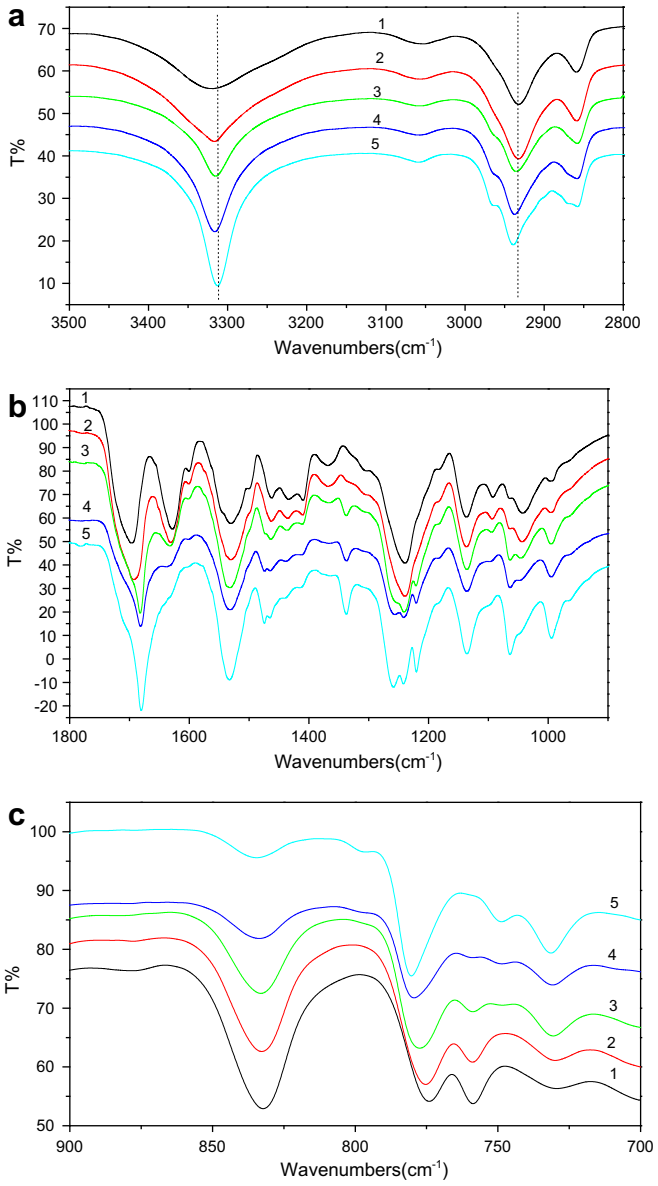

Fig. 1. The FT-IR spectras of PUPy-B series samples (1-PUPy-53; 2-PUPy-B40; 3-PUPy-B30; 4-PUPy-B20; 5-PUPy-B10) at the frequency range of (a) 3500–2800 cm^{-1}; (b) 1765–900 cm^{-1}; (c) 884–659 cm^{-1}.

at low temperature range. It implies that the phase separation consisting of soft phase and hard phase occurs in the PUPy. Similar to the microstructures changing in the SBS/PCL blends [28], as the BINA content decreases from 53 wt% to 10 wt%, the soft phase tends to change gradually from continuous amorphous phase at above 30 wt% to droplet-like dispersion phase at below 10 wt%; while the hard phase grows up from droplet-like dispersion amorphous phase at above 40 wt% to continuous semi-crystalline phase at below 30 wt%. Furthermore, it indicates that that the glass transition is influenced by the BINA unit; while the amorphous hard phase or semi-crystalline phase is resulted from the HDI-BDO unit. Because the pyridine ring of BINA unit is attached to the polyurethane chain as a pendant. The pendant pyridine ring prevents the aggregation of polymer chain. However, HDI-BDO units have great tendency to form crystals which exhibits a melting transition at ca. 165 °C [27]. Thus, HDI-BINA unit is easy to form amorphous soft phase in the samples with high fraction of BINA through the hydrogen bonding in the pyridine ring. At the same time, HDI-BDO unit as well as HDI-BINA unit also tends bind themselves to amorphous hard phase via hydrogen bonding in the urethane groups, and HDI-BDO segment even forms semi-crystalline hard phase when the fraction of BINA is low.

3.3. Dynamical mechanical properties of PUPy

Fig. 3 presents the dynamical mechanical properties of PUPy with various BINA contents. Similar to other kind of SMPs, in Fig. 3(a), it is observed that all PUPy samples have high glassy modulus (E_g), beyond 4.5 GPa at −47 °C (at the glassy state). Then a significant modulus decrease is observed during the glass transition process. Entering into the rubber state, they get very soft. Especially, when the BINA content is high, e.g. above 40 wt%, the rubber modulus (E_r) is lower than 10.0 MPa. Thus, the modulus ratio (E_g/E_r) of PUPy40 is beyond 450. However, the rubber modulus increases to above 156 MPa at 80 °C when the BINA content decreases to below 30 wt%. As a result, the modulus ratio gets smaller, closing to only 100 in the sample PUPy10. It is confirmed again that micro-phase separation occurs in the PUPy. Particularly, when the BINA content decreases to below 30 wt%, the hard phase gets clearer. It is also confirmed that the soft phase mainly is resulted from the aggregation of HDI-BINA unit; while HDI-BDO unit mainly forms the hard phase. It is consistent with the results of DSC.

In addition, in Fig. 3(b), it is also found that the two transitions appear on the Tanδ curve in the PUPy30, PUPy20 and PUPy10. They are ascribed to the glass transition of soft phase and crystal melting transition of hard phase as DSC curves described above. This is another proof for the phase separation in the PUPy. Interestingly, it

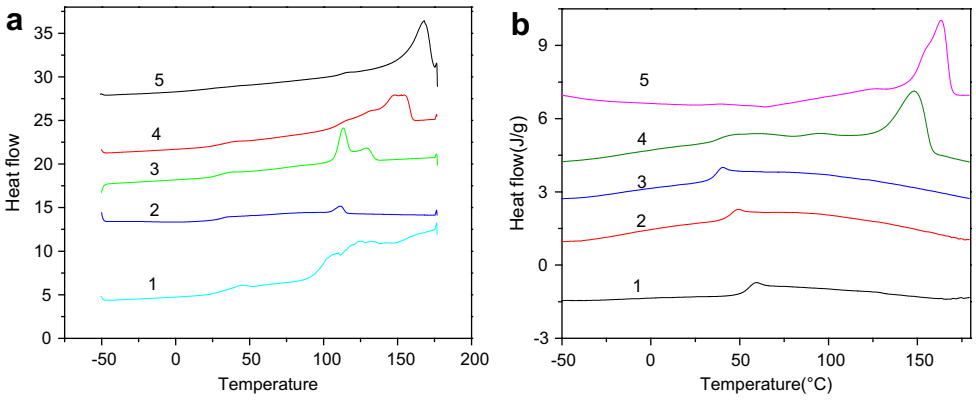

Fig. 2. DSC curves ((a) first heating; (b) second heating) of PUPy with various BINA contents: 1-PUPy53; 2-PUPy40; 3-PUPy30; 4-PUPy20; 5-PUPy10.

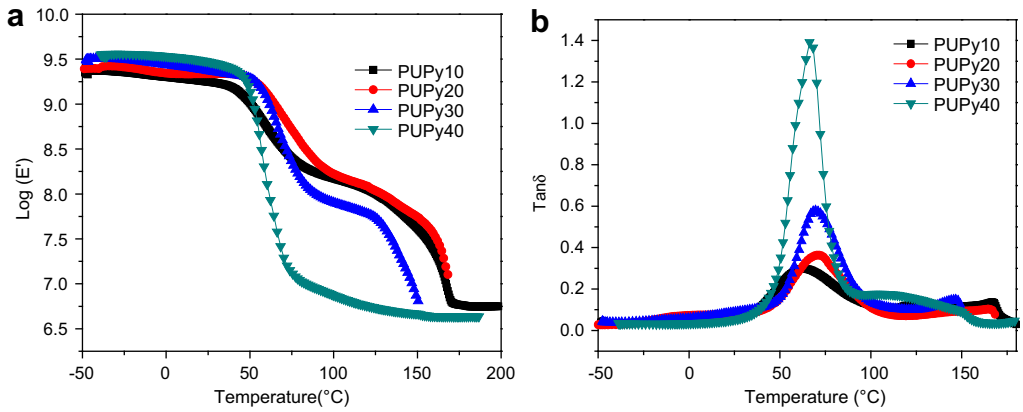

Fig. 3. DMA curves ((a) modulus; (b) Tanδ) of PUPy samples with various BINA contents.

is found that as the BINA content decreases, the maximum Tanδ gets smaller from 1.40 in the sample PUPy40 to only 0.31 in the sample PUPy10. It implies that BINA unit shows great influence on the energy loss of PUPy. That is, the higher BINA, the bigger energy loss. The reason is that rich hydrogen bonding in the pyridine ring of BINA unit results in the larger energy loss during the glass transition process.

3.4. Thermal-induced SMEs of PUPy

3.4.1. Comparison study of SMEs

The important quantities to be determined for describing shape memory properties of materials are the shape recovery (R_r) and shape fixity (R_f). The shape recovery qualifies the ability of the material to memorize its permanent shape; whereas shape fixity describes the ability of the switching segment to fix the mechanical deformation. In order to understand the shape memory behavior of PUPy, thermal–mechanical testing is performed in this study under the condition of 100% elongation at 45 °C, fixing at 20 °C and recovering at 80 °C. The strain–stress curves of sample PUPy53 comparing with the typical T_m-type-SMPU which is synthesized form PHAG, MDI and BDO [10,29], and T_g-type-SMPU which is made with PBAG, MDI and BDO [29], are presented in Fig. 4. During the testing process, we can observed that the T_m-type-SMPU shows a small stress at 60 °C due to is low hard segment content (HSC); while the T_g-type-SMPU shows a higher stress because of their

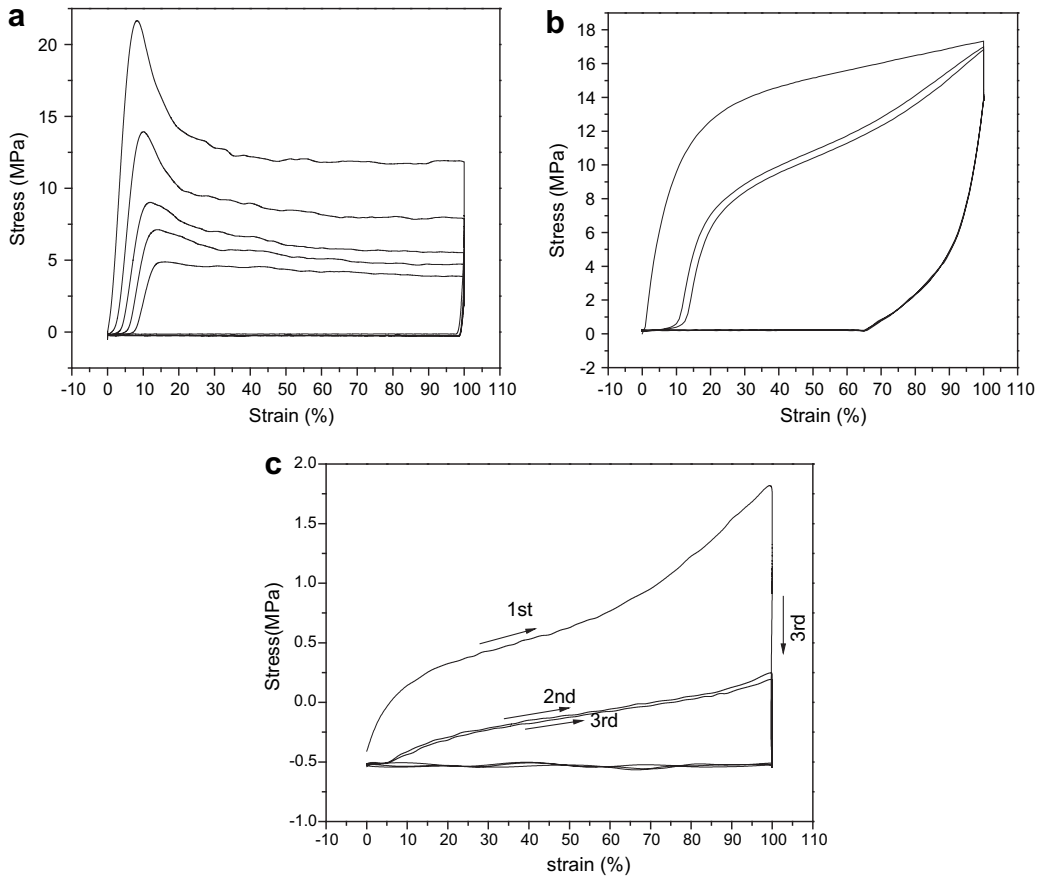

Fig. 4. Typical cyclic tensile curves of PUPy (a), comparing with T_g-type-SMPU (b) and T_m-type-SMPU (c).

higher HSC. For the PUPy, there are no soft segments, BINA unit is the main component of soft phase; and HDI-BDO forms the hard phase via the hydrogen bonding in the urethane group as described above. Thus, PUPy53 also has higher stress as they are still have a higher modulus at 45 °C.

Comparing the shape fixity, it can be found that similar to the T_m-type-SMPU, the PUPy53 has very high shape fixity, e.g. above 98%; while the T_g-type-SMPU shows small shape fixity, only about 65%. The reason is maybe that the shape fixing in the T_m-type-SMPU is resulted from the fast crystallization of PHA soft segment; while most of the deformed strain in the T_g-type-SMPU is fixed when the polymer enters into glass state. However, shape fixing in the PUPy53 mainly depends on the thermal-reversible association of hydrogen bonding in the pyridine ring. Due to the association of hydrogen bonding, polymer chain is fixed by the strong intermolecular interaction. Therefore, the strain deformed at a high temperature is easy to be fixed when the temperature cools down to below the association temperature of hydrogen bonding in the pyridine ring.

For the shape recovery, T_m-type-SMPU and PUPy53 both have a shape recovery of above 90 wt%; while the T_g-type-SMPU shows a relative low shape recovery. In addition, it is observed obviously that the shape recovery in the PUPy53 decreases as the test cyclic time increases. However, the T_m-type-SMPU and T_g-type-SMPU have a stable shape recovery from the second cycle. The reason is maybe that the hard phases of T_m-type-SMPU and T_g-type-SMPU are made with MDI and BDO. There are not only strong hydrogen bonding, but also dipole–dipole interaction and induced dipole–dipole interactions among the MDI formed hard segment [13]. Thus, the physical netpoints in the T_m-type-SMPU and T_g-type-SMPU are relative stable. In contrast, the hard phase acting as the physical netpoints in the PUPy are resulted from the ordered urethane group via hydrogen bonding in the urethane groups. Moreover, the large fraction of pendant pyridine ring in the PUPy53 prevents the aggregation of urethane unit. As the cyclic times increases, the physical netpoints are destroyed easily. Therefore, the shape recovery of PUPy decreases as the cycle time increases.

3.4.2. *Influence of BINA content on SMEs*

As we know, in the traditional SMPU including T_g-type-SMPU and T_m-type-SMPU, SMEs are influenced greatly by the molecular weight of soft segment, and content of soft segment [13]. However, in this kind of PUPy, the main composition BINA is a small unit. There is no soft segment. Thus, the SMEs are determined or influenced mainly by the BINA content. Aiming at investigate the influence of BINA content on the SMEs, a series of PUPys with various BINA contents are synthesized from HDI, BINA and BDO. Their SMEs are also investigated with thermal–mechanical testing systematically; their shape fixity and shape recovery are summarized in Table 2.

In Table 2, it is found that all the PUPy samples have very good shape fixity. Comparatively, the higher BINA content samples, e.g. PUPy53, PUPy40, have much higher shape fixity due to their large fraction of hydrogen bonding in the pyridine ring. However, the significant differences are found in the shape recovery. As the BINA content decreases, the shape recovery decreases gradually. For example, in the first cycle, PUPy53 containing 53 wt% BINA has a shape recovery of 98.5%; PUPy40 containing 40 wt% BINA has a shape recovery of 97.9%; However, when the BINA content decreases to below 30 wt%, the sample PUPy20 containing 20 wt% BINA has a shape recovery of 81%; and the sample PUPy10 containing 10 wt% BINA has a shape recovery of only 76%. At the same time, it is also found that the shape recovery in all PUPy samples decreases as the cyclic times increases as described above. Because the BINA content reflects the fraction of pyridine ring; and the shape recovery is mainly resulted from the dissociation of hydrogen bonding in the pyridine ring. These results imply that the pyridine content has great influence on the shape recovery and shape fixity. To achieve a high shape recovery, e.g. above 90%, 30 wt% BINA contents are required in the PUPys.

Table 2
Shape fixity and shape recovery for PUPy with various BINA content.

Samples	BINA (wt%)	R_f (%)	1st R_r (%)	2nd R_r (%)	3rd R_r (%)	4th R_r (%)
PUPy53	53.7	98.7	98.54	96.34	94.49	92.57
PUPy40	38.5	99.2	97.96	96.03	94.68	93.80
PUPy30	28.8	97.3	92.54	88.78	87.16	86.15
PUPy20	19.1	91.7	81.01	76.94	74.36	72.73
PUPy10	9.5	94.7	76.0	70.64	68.71	67.53

3.4.3. *The shape stability of PUPy*

Shape fixity by cyclic tensile testing is provided to characterize the capability of fixing an instant deformation. However, chain relaxation exists in all polymers. As the time goes, the free strain tends to be recovered through the relaxation process. As a result, the shape fixity may decrease as the time goes if the intermolecular action is weak. For example, Zhu *et al.* observed that the shape fixity decreases to only 60% after 24 h relaxation in the supramolecular SMPU grafting with UPy side groups. The reason was that the supramolecular SMPU contains a small fraction of UPy side groups. Therefore, it was suggested by Li *et al.* that a high fraction of H-bonding side group might provide a better SME [18]. In the PUPy, high fraction of hydrogen bonding is formed among soft phase as well as hard phase. Thus, it is expected that the strain stability of PUPy will be better than previous supramolecular SMPs.

Fig. 5 presents the strain stability of PUPy45 with 100% elongation comparing with the strain stability of PUPy53 with 100% elongation, 150% elongation and 200% elongation. It is found in Fig. 5 that the shape fixities in all samples decrease as the time goes. Especially, the strain fixity of sample PUPy45 decreases significantly from the original value (closing to 100%) to only 83% after 96 h relaxation. Comparatively, the PUPy53 has higher strain stability. Particularly, sample PUPy53 with lower elongation, e.g. 100%, tends to keep above 85% shape fixity after 40 h relaxation. However, when the elongation is too high, strain stability gets worse. For example, the strain stability of sample PUPy53 with 200% elongation decreases linearly as the relaxation time increases in particular in the first 40 h relaxation. The reason is that the PUPy53 contains large fraction of thermal-reversible hydrogen

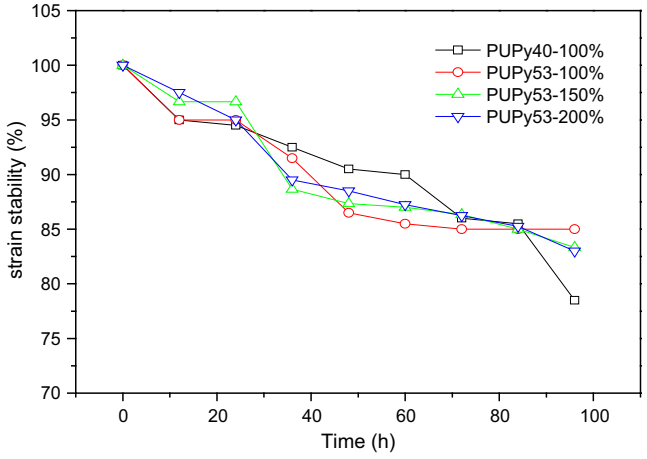

Fig. 5. Strain stability of PUPy with various BINA contents at different elongation.

bondings in the pyridine ring, which is responsible to the shape fixing. Thus, higher strain stability is expected in the PUPy with higher BINA content. However, higher elongation may also destroy the non-covalent hydrogen bonding. Then it affects the stability of hydrogen bonding in the pyridine ring. Thus, the lower elongation results in a relative higher strain stability.

3.4.4. *The temperature-dependent strain recovery of PUPy with various BINA contents*

Thermal recovery testing is used to characterize the shape recovery behaviors; and the resulted temperature-dependent strain recovery curves describe the change of strain recovery rate as a function of temperature [30]. Fig. 6 presents the temperature-dependent strain recovery curves of PUPy with various BINA contents. From the curves, it can be found that sample PUPy53 and sample PUPy40 shows the typical S-shape strain recovery process. That is, the shape changes little with increasing of temperature at the temperature range of below initial temperature (T_i) [30], e.g. 50 °C in PUPy53. However, when the temperature is raised to above T_i, the deformed strain starts to recover immediately; and abruptly strain recovery is observed in the temperature range of 50–70 °C. Thus, the shape recovery temperature (T_r) [30] is about 60 °C in the PUPy53. This temperature is very close to the T_g of soft phase as well as the dissociation temperature of hydrogen bonding in the pyridine ring. It implies that the strain recovery is resulted from the increasing chain movement due to the dissociation of hydrogen bonding. When the temperature is raised to above the recovery end temperature (T_e) [30], e.g. 80 °C, most of the deformed strains are recovered though there is still a slow strain recovery process. This shape recovery process exactly shows that the PUPy53 and PUPy40 have excellent SMEs. However, when the BINA content decreases to below 30 wt%, the final strain recovery is unacceptable. It is less than 50% in the sample PUPy10. In addition, it is also found that the higher BINA content samples like PUPy53 and PUPy45 have higher shape fixity; while the lower BINA content samples like PUPy10 and PUPy20 have lower shape fixity. These observations are consistent with the results observed by the thermal–mechanical testing. It implies that higher BINA content PUPys show better shape recovery as well as better shape fixity. Thus, the critical BINA content for PUPys exhibiting good SMEs is about 30 wt%.

3.4.5. *Strain recovery force of PUPy with various BINA content*

As we know, the driving force for shape recovery in a polymer is the elastic strain generated during the deformation. It was proposed that restoration force of SMPs can be measured as the temperature increases from room temperature to a higher temperature (above T_r) by fixed the specimen length after a procedure of deformation and fixation [31]. In an earlier study [11], we also found in the T_m-type-SMPU that the restoration stress appeared at the beginning of strain recovery, e.g. T1 = 41 °C. Then it increased to its maximum F_{max} when the temperature was raised to T2 (=60 °C), close to the end temperature of strain recovery. After the deformed strain was released completely, the recovery stress began to decrease due to the increasing temperature. In this experiment, the static stress was also recorded to characterize the restoration force upon heating with the DMA by controlling the displacement to a very small value, e.g. 0.001 mm. Fig. 7 presents the static stress curves of PUPy with various BINA contents under the elongation of 100%. Similarly, it can be observed in Fig. 7 that the static stress in the PUPy53 does not appear until the temperature is raised to above 43 °C. After that, it increases to its maximum value about 1.0 MPa as the temperature increases to ca. 50 °C. Before 58 °C, the static stress tends to be kept to above 1.0 MPa. Thereafter, the static stress is also observed to decrease with the increasing of temperature. Comparatively, it can be found that the maximum value of static stress increases significantly with the decreasing of BINA content. For example, about 2.5 MPa static stress is obtained in the sample PUPy40; while the sample PUPy30 shows a maximum static stress of 4.6 MPa at about 60 °C; and the sample PUPy20 shows a much higher static stress of above 9.0 MPa after it is heated to above 60 °C. The reason is that the rubber modulus increases with the decreasing of BINA content as observed in the DMA test. The high rubber modulus results in a higher elastic stress when the hydrogen bonding is dissociated at above T_r. Therefore, it is confirmed that the recovery energy can be stored in the deformed shape; and restoration force is an important factor to the SMMs.

3.5. *Temperature-dependent FT-IR analysis for mechanism of thermal-induced SMEs*

To investigate the mechanism of thermal-induced SMEs of PUPy, FT-IR spectra at different temperature are performed in this study. Fig. 8 presents the FT-IR spectra of sample PUPy53 at various temperatures upon heating. In Fig. 8(a), it can be found that as the temperature increases from 20 °C to 180 °C, the frequency of N–H vibration shifts from 3329 cm^{-1} to higher frequency 3349 cm^{-1}; while the frequency for the C–H vibration of pyridine ring at about 3054 cm^{-1} shifts to lower frequency at about 3041 cm^{-1}. At the same time, in Fig. 8(b), it is also observed that the frequency for

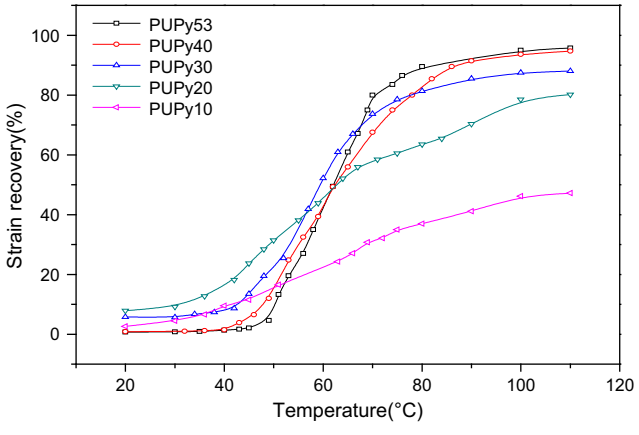

Fig. 6. Strain recovery curves of PUPy with various BINA contents.

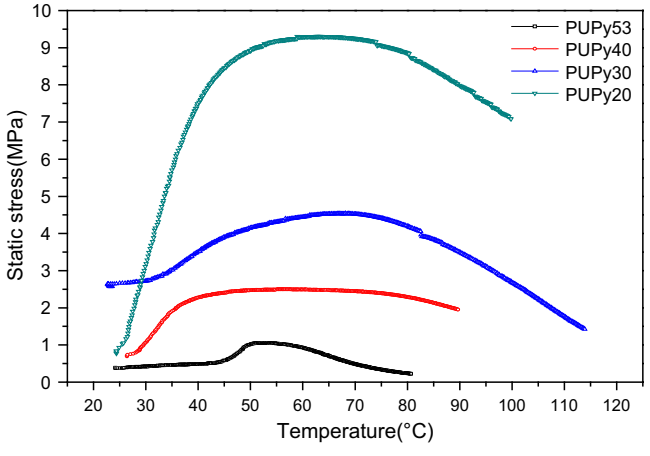

Fig. 7. Static stress curves of PUPy with various BINA content.

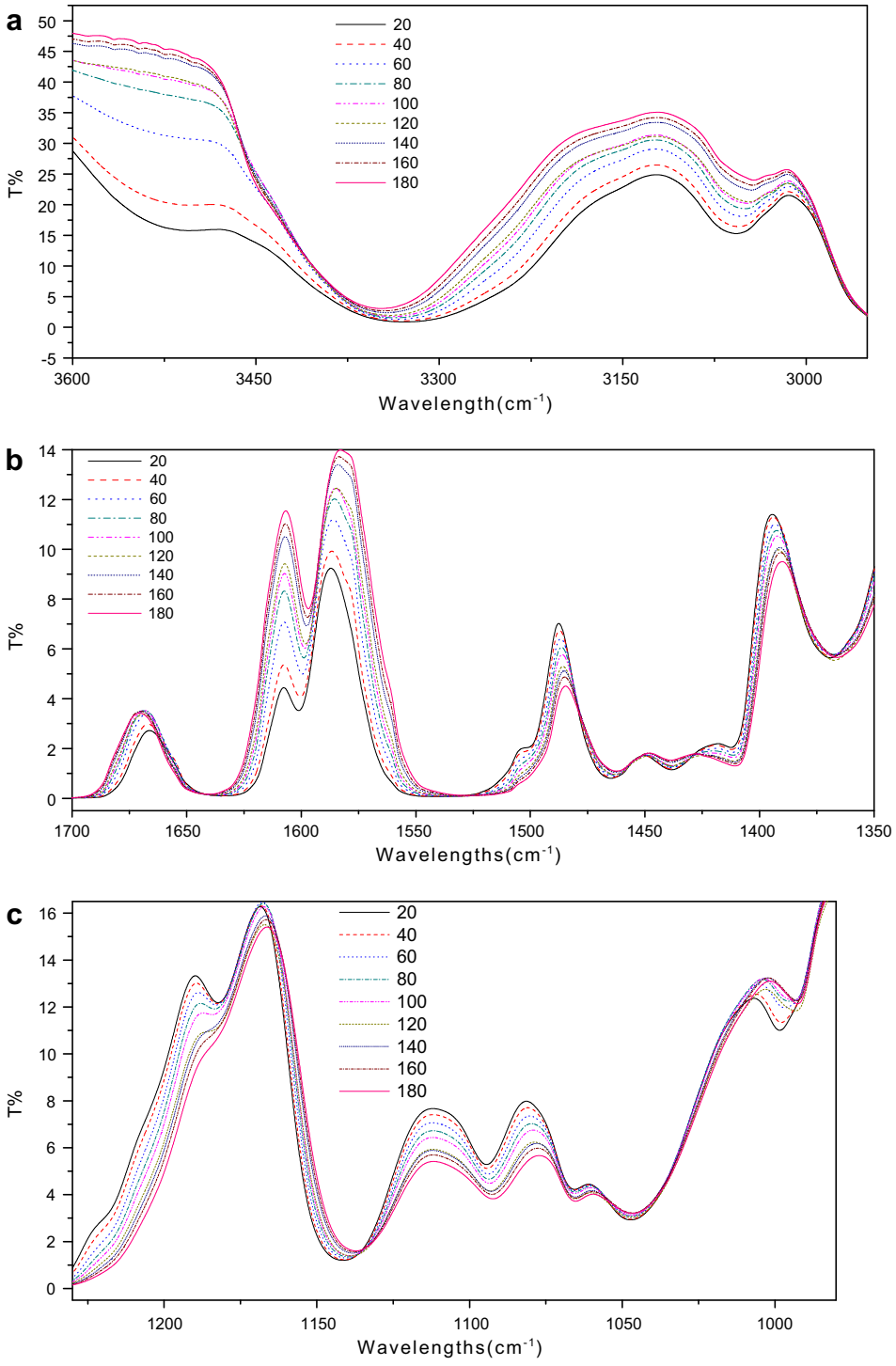

Fig. 8. FT-IR spectra of PUPy53 at various temperatures upon heating at the frequency range of (a) 3600–2950 cm^{-1}; (b) 1700–1350 cm^{-1}; (c) 1230–980 cm^{-1}.

C═O stretching vibration of urethane group shifts from 1705 cm^{-1} to 1721 cm^{-1}; and the frequency for C═O stretching vibration beside pyridine ring shifts from 1633 cm^{-1} to 1642 cm^{-1}; while the frequency for C–N–C stretching vibration of pyridine ring shifts from 1602 cm^{-1} to 1596 cm^{-1}. In Fig. 8(c), it is even observed that the pyridine ring breathing vibration frequency shifts from 999 cm^{-1} to 991 cm^{-1}. Especially, at the temperature range of 40–60 °C, the pyridine ring breathing vibration frequency shifts abruptly from 997.5 cm^{-1} to 992.5 cm^{-1}. In addition, the frequency at about 3057 cm^{-1} also decreases significantly to 3048 cm^{-1} before 60 °C; while the frequency for C–N stretching vibration at about 1183 cm^{-1} does not disappear until the temperature is raised to above 120 °C. These observations indicate that most of the hydrogen bonding in the pyridine ring dissociates at about 40–60 °C; while the hydrogen bonding in the urethane group dissociates little until the temperature is raised to above 120 °C. Therefore, the modulus of PUPy decreases significantly at the temperature range of 40–60 °C. Because the dissociation of

hydrogen bonding in the pyridine ring results in an increasing chain movement. As a result, the deformed strain recovers as the intermolecular interaction is weak. However, the whole polymer chain is still held by the hydrogen bonding in the urethane group below its dissociation temperature at about 120 °C. Therefore, the hydrogen bonding in the pyridine ring serves as the molecular switch; while the hydrogen bonding in the hydrogen bonding acts as the physical netpoints for the utilization of PUPys as SMMs.

4. Conclusions

A series of PUPys were synthesized from BINA, HDI and BDO. Then the structure and morphology of PUPys were investigated using the FT-IR, DSC and DMA; and thermal-induced SMEs were particularly studied systematically in this paper. Finally, the following conclusions can be summarized:

1) Strong hydrogen bonding is formed in the urethane group as well as in the pyridine ring. As the BINA content decreases, the fraction of hydrogen bonding in the urethane groups increases; while the fraction of hydrogen bonding in the pyridine ring decreases. Moreover, the strength of hydrogen bonding in the urethane group gets stronger; while the strength of hydrogen bonding in the pyridine ring get weaker.
2) DSC and DMA results show that phase separation consisting of soft phase and hard phase occurs in the PUPy. As the BINA content decreases from 53 wt% to 30 wt%, the T_g of soft phase moves to low temperature; while the soft phase tends to disappear; and the HDI-BDO tends to form semi-crystalline hard phase in the samples with below 30 wt% BINA content. Moreover, significant modulus decrease is observed on the glass transition process; and the rubber modulus increases with decreasing of BINA contents.
3) Thermal–mechanical testing and temperature-dependent strain recovery show that the lower limit of BINA content for PUPys exhibiting good SMEs is 30 wt%. As the BINA content decreases, the shape fixity decreases a little; while the shape recovery decreases significantly. In addition, strain stability is better in the higher BINA content PUPy with lower elongation; and the shape recovery force increases with the decreasing of BINA content.
4) Finally, the temperature-dependent FT-IR spectra support that the hydrogen bonding in the pyridine ring serves as the molecular switch; while the hydrogen bonding in the hydrogen bonding acts as the physical netpoints for the utilization of PUPys as SMMs.

Acknowledgements

This work was financially supported from the Ph.D. studentship of Hong Kong Polytechnic University. The authors also would like to thank Prof. Jean-Marie Lehn, the Nobel Prize Laureate in 1987, for his guidance.

Appendix. Supplementary material

Supplementary data associated with this article can be found, in the online version, at doi:10.1016/j.polymer.2009.11.034.

References

[1] Ratna D, Karger-Kocsis J. Journal of Materials Science 2008;43(1):254–69.
[2] Behl M, Lendlein A. Soft Matter 2007;3(1):58–67.
[3] Yuan Z, Ji B, Wu LB. Acta Polymerica Sinica 2009;(2)::153–8.
[4] Hollander SD, Assche GV, Mele BV, Prez FD. Polymer 2009;50(19):4447–54.
[5] Lendlein A, Jiang HY, Junger O, Langer R. Nature 2005;434(7035):879–82.
[6] Cho JW, Kim JW, Jung YC, Goo NS. Macromolecular Rapid Communications 2005;26(5):412–6.
[7] Jiang BH, Zhou WM, Liu Y, Qi X. Materials Science Forum 2003;426–432(Pt. 3): 2285–90.
[8] Huang WM, Yang B, An L, Li C, Chan YS. Applied Physics Letters 2005;86(11):114105.
[9] Liu GQ, Ding XB, Cao YP, Zheng ZH, Peng YX. Macromolecular Rapid Communications 2005;26(8):649–52.
[10] Chen SJ, Hu JL, Liu YQ, Liem HM, Zhu Y, Liu YJ. Journal of Polymer Science Part B: Polymer Physics 2007;45(4):444–54.
[11] Chen SJ, Cao Q, Jing B, Cai YL, Liu PS, Hu JL. Journal of Applied Polymer Science 2006;102(6):5224–31.
[12] Ji FL, Hu JL, Li TC, Wong YW. Polymer 2007;48(17):5133–45.
[13] Lee BS, Chun BC, Chung YC, Sul KI, Cho JW. Macromolecules 2001; 34(18):6431–7.
[14] Zhang S, Yu ZJ, Govender T, Luo HY, Li BJ. Polymer 2008;49(15):3205–10.
[15] Liu GQ, Guan CL, Xia HS, Guo FQ, Ding XB, Peng YX. Macromolecular Rapid Communications 2006;27(14):1100–4.
[16] Liu GQ, Ding XB, Cao YP, Zheng ZH, Peng YX. Macromolecules 2004; 37(6):2228–32.
[17] Luo HY, Liu Y, Yu ZJ, Zhang S, Li BJ. Biomacromolecules 2008;9(10):2573–7.
[18] Li JH, Viveros JA, Wrue MH, Anthamatten M. Advanced Materials 2007;19(19):2851–5.
[19] Zhu Y, Hu JL, Liu YJ. European Physical Journal E 2009;28(1):3–10.
[20] Chen SJ, Hu JL, Yuen CW, Chan LK. Polymer 2009;50:4424–8.
[21] Chen SJ, Hu JL, Yuen CW, Chan LK. Materials Letters 2009;63(17):1462–4.
[22] Cao Q, Chen SJ, Hu JL, Liu PS. Journal of Applied Polymer Science 2007;106(2):993–1000.
[23] Brunette CM, Hsu SL, Macknight WJ. Macromolecules 1982;15(1):71–7.
[24] Ambrozic G, Zigon M. Acta Chimica Slovenica 2005;52(3):207–14.
[25] Luo N, Wang DN, Ying SK. Macromolecules 1997;30(15):4405–9.
[26] Robert WS, Stuart LC. Macromolecules 1973;6(1):48–53.
[27] Korley LTJ, Pate BD, Thomas EL, Hammond PT. Polymer 2006;47(9):3073–82.
[28] Zhang H, Wang HT, Zhong W, Du QG. Polymer 2009;50(6):1596–601.
[29] Chen SJ, Hu JL, Liu YQ, Liem HM, Zhu Y, Meng QH. Polymer International 2007;56(9):1128–34.
[30] Li FK, Hou JN, Zhu W, Zhang X, Xu M, Luo XL, et al. Journal of Applied Polymer Science 1996;62(4):631–8.
[31] Ping P, Wang WS, Chen XS, Jing XB. Biomacromolecules 2005;6(2):587–92.